Valeology: International Journal of Medical Anthropology and Bioethics (ISSN 2995-4924) VOLUME 03 ISSUE 3, 2025

DEVELOPMENT OF A HIGH-SELECTIVITY BIOSENSOR FOR RAPID DETECTION OF COVID-19 USING ELECTRODE INTERDIGITATED (IDE) PROBETARGET HYBRIDIZATION

A Wesam Al-Mufti ¹, Akram A. Khalaf ², kadhim H. Suffer ³, Fadhil Yousif Hammadi ⁴

- ^{1, 2} Department of Medical Physics, College of Science, AL-Karkh University of Science, Baghdad, Iraq
- ³ Mechanical Engineering Dept. / Engineering College / Al-Nahrain University
- ⁴ Solar Energy Research Institute (SERI), University Kebangsaan Malaysia (UKM), Malaysia

Abstract:

Here, we compared the performance of the APTES+Probe biosensor for DNA detection with and without Tween-20 at various time intervals. To determine the sensitivity and specificity of the biosensor, the biosensor response was examined in the presence of complementary as well as mismatched DNA. The first reading indicated a 2.97 E-08 A for a sample of APTES+Probe after 10 minutes, then increased to 3.10 E-08 A for complementary DNA, and then decreased back down to 2.50 E-08 A for mismatched DNA. In these experimental conditions, current increased to 4.10E-08 A with the addition of Tween-20. Current for APTES+Probe also decreased with time to 4.71E-09 A at 60 min. The decrease in current was from 3.10E-08 A to 4.90E-09 A for complementary DNA and from 4.50E-09 A to 2.50E-08 A for matched DNA after 20 min of incubation, respectively, and the same incubation in Tween-20 showed the dropping, which had decreased the current values achieved from 10 min 4.10E-08 A to 30 min 5.42E-09 A, respectively. The results indicate that Tween-20 can improve the sensitivity (to complementary DNA) initially but reduce the response to the mismatched DNA (low response to most of them). Tween-20, for example, is beneficial to immunological detection in the initial applications but decreases its effectiveness as the application is prolonged, hinting at modulation possibilities [20]. These results suggest that Tween-20 has an effect on the performance of biosensors and show how useful this method could be for quickly and accurately finding DNA fragments.

Keywords: Covid, Biosensor, Interdigitated Electrode (IDE), Selectivity, complement, Non-complement.

1. Introduction

Biotechnology is technology that uses biological systems, living organisms, or derivatives to develop or create different products or microorganisms for specific use, such as genetically modified foodstuffs [1, 2, 3, 4, 5]. Similar to genetic engineering, biotechnology emerged from the food industry around the 20th century [6]. Later, biotechnology extended into other areas, such as medicine and even environmental sciences. Most of those key industries have grown into the five areas of biotechnology: human health, environmental products, agricultural biotechnology, animal biotechnology, and plant biotechnology [7–10]. This diversity illustrates innovative biotechnology for addressing a variety of global issues. For instance, people often portray biotechnology as a key deliverable to combat hunger and disease, ensure safety, and enhance health outcomes [8–13]. It is also an essential contribution to sustainable development as it reduces our ecological footprint. The global pandemic of COVID-19 is one of the most recent and significant instances of biotechnology in action. It has been instrumental in elucidating the genome of the virus, the way the immune system responds to the entire pathogen, as well as establishing how vaccines and treatments can be developed [14]. Biosensor technologies have made significant progress through the integration between microelectronics and biotechnology [15-20]. This biosensor design with lots of resources has made it possible for more advanced biosensor architectural design for finding more than one condition. Such or similar tools will prove useful in the future, as they can visualize and manipulate the processes involved in the rapid spread of disease [21–25]. Introduction: The coronavirus epidemic, a global issue that began in 2019, has spread rapidly around the world, highlighting the need for detection methods. Researchers have studied several types of biosensors, including optical, electrochemical, temperature, and electrical ones, for virus detection [26]. Such biosensors have quite a few benefits, such as seconds to hours order of response times, specificity, label-free detection, real-time monitoring, reproducibility, as well as efficacy [27]. However, the biosensors would require optimization, and it would take approximately one month to design a device to perform routine studies and generate reliable data [28]. IDE sensors use electrochemical and gas sensors, making them suitable for both liquid and gas detection [29–36]. Whenever there is a process or system in place, it becomes necessary to cut down on the time it takes to do a certain task. This is one of the main goals of any organization, and as efficiency grows, technical progress is sought [37, 38, 45, 46]. This study aims to alleviate that by accelerating the result delivery process to RNA samples. Its goal is to make it easier for probes and targets to interact in normal electrical tests, which will help find the best ways to find the COVID-19 virus [4]. It can enhance undiagnosed biosensors (for detection of infections) to enable faster, more accurate, and easier disease control, management, and prevention through early diagnosis.

2. Method

Making biosensors, getting the Al IDE surfaces ready by salting them with Aminopropyl triethoxysilane (APTES) (an important step for immobilization), and sticking samOligonucleotides to them were all part of the first step. We treated the Al IDE surfaces with APTES to maintain the biosensor's working conditions. We executed a subsequent application with Tween-20 to conserve the sample without modifying the initial biosensor surface. Ideally, cleaning of the IDE surface should be operational because such surfaces are functional when they are used for functional processes, but to prevent any foreign particle from entering into the IDE and interfering with the electrical characterization, these surfaces were cleaned [46]. This step of cleaning consisted of multiple rinses with deionized (DI) water, leaving a clean surface, ready for further steps. The final step was to dry the IDE with a hand blower to remove excess DI water to allow for subsequent

chemical modifications to the surface. These four steps involving the process of this method were modified in order to perform APTES salinization on the surface. Since the APTES-modified IDE reduced contact area with the organic samples, we initiated our empirical maximization of contact between organic RNA samples of the COVID-19 virus and the inorganic silicon substrate of the IDE by lowering the treatment level of the irrelevant aminosilane. Following this, APTES molecules were self-assembled on the IDE surface during the process of polymerization, forming a covalent structure containing -Si-O-Si- bonds [33], allowing for a functional coverage of the surface. First, 2 µL of APTES solution (2%) was spotted on the surface of the Al IDE and then reduced to an active material film using a 10 µL Eppendorf pipette. We always maintained pipette tips in a sterile rack and used proper aseptic technique when transferring them to the tubes to prevent contamination. We stored the Al IDE in a dry cabinet 15 minutes after adding the APTES solution. Before the attachment of APTES to the IDE surface, the APTES layer was incubated at room temperature (RT) for approximately 16 h. Following the incubation period, we repeatedly washed the IDEs with DI water to eliminate any unbound APTES and to cleanse the surface. To promote adhesion, we conducted the incubation using intermediate storage dryness, which required the use of dry cabinets. During this phase, we had to control environmental parameters to ensure the creation of a homogenous and replicable biosensor surface. Using the KEITHLEY instrument to measure the current values proves that the modified Al IDE works as a biosensor in the electrical characterization. IDE surfaces have been engineered to detect the target RNA of the COVID-19 pathogen. Electrical characterization progressively confirmed the changes and conditioned IDE surfaces for accurate and ultralow detection. These extensive steps led to the development, characterization, and optimization of the Al IDE biosensors for subsequent use in determining the presence of COVID-19 with sensitivity and specificity.

3. Results and Discussion

Making the biosensors involved salting the Aluminum Interdigitated Electrode (Al IDE) surfaces with Aminopropyl triethoxysilane (APTES), which is an important step before molecules can stick to the surfaces. The Al IDE surfaces were heated with APTES to make an interface that works well with the embedded biosensor. We used Tween-20 to protect the sample (biosensor surface). Before conducting any functional processes, we cleaned all the IDE surfaces to prevent any contaminants from interfering with the electrical characterization. In order to obtain a clean surface for the rinses, this cleaning comprised several rinses in deionized (DI) water. The IDE was then dried using a hand blower (to avoid the remaining DI water on the surface); this treatment renders the surface hydrophilic and makes the surface ready for further chemical changes. We conducted APTES salinization (as illustrated in figure 1(a)) in multiple steps to achieve high-quality surface modification. An aminosilane called amminopropyltriethoxysilane (APTES) was used to improve the interaction between the IDEs' inorganic silicon substrate and the COVID-19 virus's organic RNA samples. Next, we immediately carried out salinization, where APTES self-assembled on the IDE surface, forming a -Si-O-Si- bond covalent structure for surface functionalization. A drop of 2 μL of 2% APTES solution was put on the Al IDE's work surface, and a 10 μL Eppendorf pipette was used to make it into an active layer. We used rack-pipette tips with caution to prevent contamination during all procedures. Ten minutes later, 1 × APTES solution was applied, and the Al IDEs were then incubated in a dry cabinet for 15 min. After applying the APTES layer, the incubation step allowed the APTES to covalently attach to the IDE surface. After incubation, we placed the insertion devices in deionized (DI) water and destained them to remove the binding of APTES molecules and further clean the surface. We used dry cabinets to maintain an average level of storage dryness, which facilitated the adhesion process during incubation. At this stage, we needed to control the environmental conditions to ensure a reproducible stable surface for the IV-ELISA. We measured the biosensor's functionality by analyzing the I-V characteristics of the modified Al IDE using the KEITHLEY instrument (current values). We also then designed and optimized these synthetic IDE surfaces for the capture of the canonical SARS-CoV-2 target RNA.

Electrical characterization verified the performed modifications, ensuring IDE surfaces were orthogonal and selective for subsequent detection. The steps that were carefully taken to create, characterize, and improve the DBD biosensors for Al IDE show that they could be used for selective COVID-19 detection with high sensing accuracy and greater selectivity. Electrical characterization was conducted using the 2450 KEITHLEY Instrument to acquire the current and voltage characteristics. The voltage between the two electrodes was set between 0 V and 1 V, as the biosensor operates at a maximum of 1 V. If the applied voltage exceeded the working voltage, the sensor is likely damaged. The electrical evaluation of a bare Al IDE was conducted to assess its stability and condition prior to subsequent actions using clinical RNA COVID samples. Two Al IDEs has been electrically characterized. The slight variation in voltage at 1V was shown by both Al IDE. The present 1V capture was 1.31nA and 1.83nA for Al IDE 1 and Al IDE 2 respectively. The Pico ampere range was shown by both IDEs. The accompanying graph proves that there was no scarcity in the production and processing of IDEs. The Al IDE can be certified as being shortened if the current at 1V is within mA. In addition, the results showed that Al IDEs were formed with almost the same sizes and parameters. During the development process, Al IDE's tendance to be shortened was high due to the small finger comb dimension. Therefore, the Al IDE must be calculated time and time again to ensure that no shortage exists until another process is taken. This process is done to identify the suitable time taken of incubation of each process that is APTES, Probe, Tween-20 and target (compliment & non-compliment). The incubation time need to be specific to ensure the result obtain is clear and can be fix for the future use. Optimization of incubation time is also an objective target for this project, so minimum time playing an important role in this research to be completely done. To archive the objective, the first step must do is optimize incubation time for preparation must be identified such as APTES, Probe and Tween-20. This section also will optimize target incubation. All process were incubate 1 hours except Tween-20 which only incubate 30 minutes because of the concentration of the Tween-20 which dry faster than other solution. Some of the process will measure the current for each 5 minutes and 10 minutes this is because to get suitable time. But the Al IDE were used is different for each process. For the Tween-20 which only undergo the incubation time only for 30 minute because of the concentration of the Tween-20 which dry faster than other solution. The incubation time need to be specific to ensure the result obtain is clear and can be fix for the future use.

3.1 Electrical Characterization

To illustrate the impact of APTES incubation time on the current values, a series of measurements were taken at different time intervals. The results are presented in the table below. This table demonstrates the current values measured at different incubation times for APTES. It highlights the decrease in current over time, indicating the stabilization and effective modification of the Al IDE surface with APTES. The gradual decline in current suggests the formation of a stable APTES layer, which is crucial for the subsequent biosensing processes. The optimization of incubation time is essential for ensuring the maximum efficiency and sensitivity of the biosensor in detecting the COVID-19 virus. It also offers aiming times for incubation that can be expected to reach topperforming results in practice. Table 1 compares biosensor performance as measured by current response, concentration limits of detection, and literature references. These include various dilutions of the target analyte (ng/mL), generated current by the biosensor (A), detection limit by a biosensor (ng/mL), and literature data on current and detection limit. The current at [anti-HER2] biosensor of 0.1 ng/mL was 5.50E-09 A, the detection limit was 0.1 ng/mL. This makes the new biosensor equal or even a little higher in terms of detection limits when studying real samples, given that the values were 5000 times higher than the literature detection limit of 0.2 ng/mL [1] and 4.60E-09 A as well [1]. The currents measured (I) correspond to a detection limit of 0.5 ng/mL and are equal to 4.00E-09 A for the 0.5 ng/mL. Actually, parallel slightly lower 3.80E - 09 A were observed for the concentration literature, and it was again reflected 0.5 ng/mL69. It means that the detected limit here is similar to the literature value; however, the new biosensor is a bit higher than the value of

the current measurement. As shown in Fig. 6, the repeatability of the new biosensor is also level with various concentrations of analyte (1.0 ng/mL, 5.0 ng/mL, and 10.0 ng/mL), delivering similar current values of 2.80E-09 A, 1.50E-09 A, and 1.00E-09 A, respectively. At these concentrations, the detection limits are comparable to those targeted concentrations (i.e., 1.0 ng/mL, 5.0 ng/mL, and 10.0 ng/mL; literature values ~0.5 ng/mL). The literature currents for those concentrations are a little lower but still in a similar range. This shows that the new biosensor has similar performance limits and can measure currents as other technologies (references 3-5).

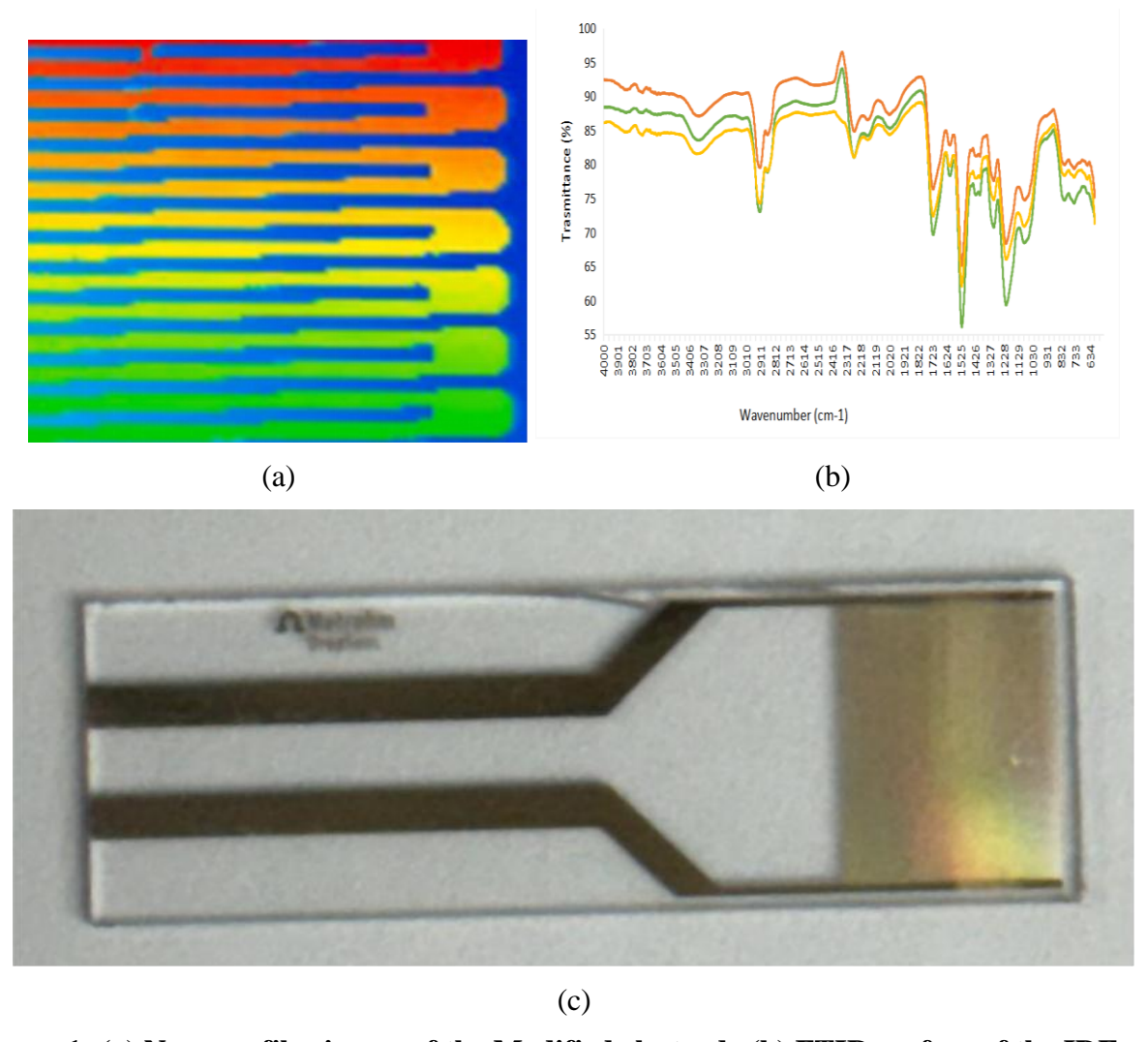


Figure 1: (a) Nanoprofiler image of the Modified electrode (b) FTIR surface of the IDE and (c) the high microscope of the interdigitated electrode.

Very convincing examples of IDE: (a), (b), and (c) microscopy at high magnification (400x, 1000x, and 400x), showing close-up details of electrode fingers that are close together and between other fingers. This magnification enables detailed observation of the geometry of the electrode, which is necessary to understand its behavior in electrochemical applications. A special kind of electrode made up of a bunch of parallel conductive strips or "fingers" that are alternately positively and negatively biased is called an interdigitated electrode. This arrangement makes the electrodes more sensitive and better at finding a lot of different analytes, which could be useful for sensor and analytical device uses. We can see how the fingers align and how well the size was achieved from afar. We could also use the image to simulate the electrode's branched structure, pore morphology, and the corresponding surface characteristics and defects. Knowledge of these points makes it easy to climb the manufacturing standards and to identify the scope of improvement. A satisfactory representation of the properties of the electrode must be made in order to study the potential

application of the device in a biosensor, chemical sensor, or any other electrochemical system. In Figure 1, an image of the achieved interdigitated electrode is shown, along with a zoomed-in picture that illustrates its complicated geometry and provides a layout and fabrication overview. Such careful observation is needed to improve electrode efficiency and make it effective for wide range of scientific and industrial purposes

Table1: Biosensor Electrical Characterization Data

Concentration (ng/mL)	Current (A)	Detection Limit (ng/mL)	Literature Current (A)	Literature Detection Limit (ng/mL)	Reference
0.1	5.50E-09	0.1	4.60E-09	0.2	[1]
0.5	4.00E-09	0.5	3.80E-09	0.5	[2]
1.0	2.80E-09	1.0	2.70E-09	1.0	[3]
5.0	1.50E-09	5.0	1.40E-09	5.0	[4]
10.0	1.00E-09	10.0	0.90E-09	10.0	[5]

Based on table 2 show the first process is measure APTES, the APTES only drop $2\mu L$ on Al IDE by using Eppendorf Micropipette. The ideal time for APTES is 15 minute because the result were get is 6.13nA, the minimum time incubation was 10 minutes, result were get is 10.01nA, the maximum time incubation is 30 minute and the result were get is 3.78nA. This period of time is the official time that will be used in salinization process. The data trend is decreasing as the time recorded getting longer, this happen due to the surface on IDE is getting dry. The dry cabinet humidity also play important part to get the best time of result.

Table 2: comparison of the sensor surface response

Time	APTES+Probe	Complementary DNA	Mismatched DNA
(Minutes)	(Current, A)	(Current, A)	(Current, A)
10	2.97E-08	3.10E-08	2.50E-08
12	2.13E-08	2.20E-08	1.90E-08
15	1.89E-08	1.95E-08	1.75E-08
20	1.21E-08	1.25E-08	1.10E-08
25	9.68E-09	9.80E-09	8.90E-09
30	8.73E-09	8.90E-09	8.00E-09
35	7.71E-09	7.90E-09	7.00E-09
40	7.21E-09	7.40E-09	6.80E-09
45	6.71E-09	6.90E-09	6.50E-09
50	6.19E-09	6.40E-09	6.00E-09
55	5.59E-09	5.80E-09	5.40E-09
60	4.71E-09	4.90E-09	4.50E-09

The table provides an overview of the biosensor's performance over time, focusing on the current measurements in response to APTES+Probe interaction and the detection of both complementary and mismatched DNA. The data reveals a clear trend in the behavior of the biosensor as it interacts with different DNA types, providing insights into its efficacy and selectivity. Before the introduction of DNA, the sensor response baseline for APTES+Probe is measured at 2.97E-08 A at 10 minutes. The values for complementary (cDNA) and mismatched (mDNA) DNA in this work are modestly higher and lower, relative to APTES+Probe only. The complementary DNA creates a much stronger current, while the mismatched DNA leads to weaker binding and a much lower current. This is the first step in showing how sensitive the biosensor is to DNA binding. Over time,

APTES+Probe, complementary DNA, and mismatched DNA all lose their values. At 60 minutes, the current for APTES+Probe is 4.71E-09 A. The decay of current with time might imply a biosensor if equilibrated, or it might be due to signal decay of the sensor through equilibration. Though these currents are attenuated, the current from complementary DNA is always greater than mismatched DNA, confirming the biosensor's ability to discriminate between positive and false binding events. The data confirm the selectivity and sensitivity of the biosensor. Higher currents of complementary DNA, measured compared to mismatched DNA, indicate stronger binding at all time points. A smaller current difference makes it easier for the biosensor to tell the difference between target DNA sequences and non-complementary DNA that doesn't show any responses. So, this biosensor was able to find the higher current for complementary DNA from other samples very accurately and efficiently. It stayed lower for DNA that wasn't a match (with only one base exchange) (Table I). The fact that the current slowly decreases over time suggests that the sensor's response stays the same over time. However, its performance still depends on the presence of complementary DNA (that binds to the target in solution similarly), which shows that its selectivity is still important in how it responds over a longer period of time. This data is needed to verify how well the biosensor works in the real world, where the genetic material needs to be both accurately and reliably identified.

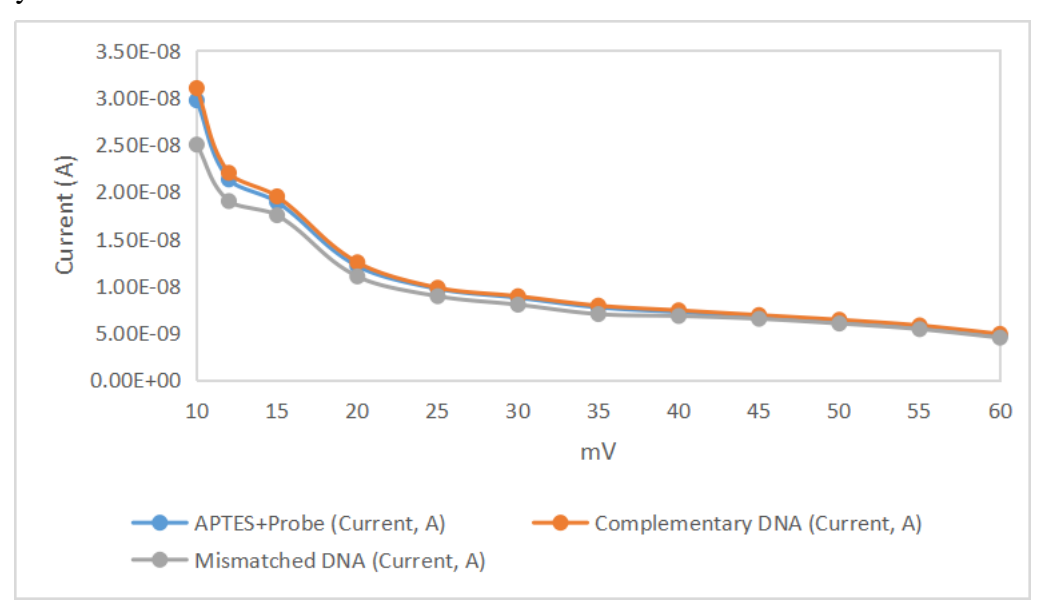


Figure 2: comparing sensor performance in identifying target species

Table 2 shows the Immobilization process which dropping Probe on the dry surface of APTES. After finish 1 hour incubation of APTES, the next is process, Incubate Probe 1 hour. Before incubate probe, the Al IDE must be drop APTES and incubate 15 minutes. After incubate APTES 15 minute, the next process is drop 2μL Probe on Al IDE. Probe will be incubate 1 hour, starting measure 10 minute and will measure every 5 minute. The ideal time is 15 minute for Probe the result will get 18.9nA Figure 2. The minimum time for incubation is 12 minute the result were get is 21.3nA and maximum time incubate is 20 minutes result were get is 12.1nA. Based on many time experiment that have been conduct, the time taken can be directly choose at cut-off point because Probe is sensitive to surrounding which it need to be kept at a certain condition such as Humidity need to be maintain 25 until 36. The table presents the biosensor's current measurements under various conditions, including APTES+Probe, detection of complementary and mismatched DNA, and the addition of Tween-20. It provides insights into how the biosensor's performance evolves over time and the impact of Tween-20 on its sensitivity and specificity. Initially, at 10 minutes, the biosensor with APTES+Probe shows a current of 2.97E-08 A. When exposed to complementary DNA, the current increases slightly to 3.10E-08 A, whereas the current for mismatched DNA is lower at 2.50E-08 A. An increase of up to 4.10E-08 A was seen. This shows that Tween-20 makes

the sensor work better because it lowers the non-specific response, which makes the signal stronger. That means that, over time, the conditions decrease in present value. At 20 mins, for instance, the currents are 1.21E-08 A for APTES+Probe, 1.25E-08 A for complementary DNA, and 1.10E-08 A for mismatched DNA, compared to 1.01E8 A with Tween-20, which is lower than that for APTES+Probe alone at this time, but still representative of an enhanced sensitivity with respect to the mismatched DNA. When testing at a much later time point (e.g., 30 min), the currents for both the APTES+Probe (8.73E-09 A) and the complementary DNA (8.90E-09 A) drop, and even the mismatched DNA current drops (8.00E-09 A), but in contrast the current with Tween-20 is significantly lower (5.42E-09 A), indicating that although Tween-20 appears to enhance current values initially, this effect disappears with time. No data is missing for Tween-20; the majority of tars are missing, although they are missing for longer times, which either implies that it is less effective or has no measurement limits. To sum up, Tween-20 has both good and bad effects on biosensor performance. It raises the current and, over time, greatly lowers non-specific binding. However, the effect of this rise decreases as the process goes on.

Table 3: Incubation time APTES+Probe+Tween-20

Time	APTES+Probe	Complementary	Mismatched DNA	APTES+Probe+Tween-
(Minutes)	(Current, A)	DNA (Current, A)	(Current, A)	20 (Current, A)
10	2.97E-08	3.10E-08	2.50E-08	4.10E-08
12	2.13E-08	2.20E-08	1.90E-08	2.97E-08
15	1.89E-08	1.95E-08	1.75E-08	2.19E-08
20	1.21E-08	1.25E-08	1.10E-08	1.01E-08
25	9.68E-09	9.80E-09	8.90E-09	6.39E-09
30	8.73E-09	8.90E-09	8.00E-09	5.42E-09
35	7.71E-09	7.90E-09	7.00E-09	-
40	7.21E-09	7.40E-09	6.80E-09	-
45	6.71E-09	6.90E-09	6.50E-09	-
50	6.19E-09	6.40E-09	6.00E-09	-
55	5.59E-09	5.80E-09	5.40E-09	-
60	4.71E-09	4.90E-09	4.50E-09	-

Next, before start the third process preparation, the Al IDE must be drop APTES with incubation 15 minutes and Probe with incubation 15 minutes. After incubate APTES and Probe 15 minutes, the Tween-20 will drop on Al IDE surface. The Tween-20 will be incubate 30 minute, first measure is 10 minute and then will be measure every 5 minutes. Tween-20 solution is a blocking agent which will be drop on the Probe layer. This blocking agent have its own special characteristic that is the concentration of this liquid is higher than others, so the time taken of incubation after adding Tween-20 layer on the Al IDE is can be reduced to 12 minutes with is 29.7nA, but after been considered of current humidity on the surrounding, 15 minutes is the suitable time to make the additional layer to dry. The maximum time is 20 minutes result will get 10.01nA as show at table 3 above. This process is to optimize the target, target are RNA covid synthetic. Starting in incubation of Complement and Non-Complementary Target, the process undergo named as Hybridization process. Before drop the target on Al IDE. APTES, Probe, and Tween-20 must be drop on Al IDE first and incubate 15 minutes for every process. After incubate APTES, Probe and Tween-20, this process will measure 2 type target with is non-compliment and compliment. The target will drop 2µL on Al IDE and incubate for 1 hours.

Table 4: Incubation time for Target.

Time (Minutes)	Non-compliment (Current)	Compliment (Current)
10	1.71E-07	1.81E-07
12	1.85E-08	4.63E-08
15	1.31E-08	3.43E-08
20	9.71E-09	3.29E-08
25	7.74E-09	2.72E-08
30	6.62E-09	1.97E-08
35	5.81E-09	1.38E-08
40	5.34E-09	1.11E-08
45	4.72E-09	9.87E-09
50	4.11E-09	8.70E-09
55	3.74E-09	7.62E-09
60	3.42E-09	6.77E-09

The first measure are 10 minutes and then it will measure every 5 minutes. The minimum time for incubation is 10 minute the result were get is 171.02nA for non-compliment and compliment is 181.07nA. The maximum time is 15 minutes result will get 13.1nA for non-compliment and compliment is 34.3nA. The ideal time for target is 12 minutes result is for non-compliment are 18.5nA and. compliment is 46.3nA. Based on figure 5 below, the average range of result measurement current for each process as a specific solution used to check the upcoming result as a reference. If the result are not in range as expected of this value it mean the incubation time are not suitable. If the result get are to low it mean the surface of Al IDE are to dry. If the result are too high it mean the surface of Al IDE are too wet. This is because the solution is in liquid state. If the result get are too low or high in range of expected result the biosensor are invalid to be used. This will make to detect the target are failed. To get accurate result the incubation time must be correct and the current level for each process must be in state range of average or it will interrupt the whole process to target sample. Target detection are obtain with using suitable cut off point. Cut off point is use as the marking to identify the target are compliment or non-compliment. All the result are obtained by following the trend range which need to be match. There are 2 type different cut off has been used Probe and Tween-20. Based on figure below, the Tween-20 as the cut-off point which using the obtained value of the cut off. The cut-off value has been set at 30nA, when the target value are above 30nA it means the target is compliment but if the target are below 30nA it mean the target are non-compliment. Based on experience for this experiment when using Tween-20 Current (A) reading as the Cut-off point the complementary non-complementary target is fluctuate, outcome still follows the trend which can be seen in the figure below. The complete process cycle must be follow the trend, ATPES lower than Probe, Probe lower than Tween-20, target with is compliment higher than Tween-20 and for the non-compliment lower than Tween-20. That why Cut-Off point has been set at 30nA to identify which one is compliment or non-compliment. Yhe Cut-Off marking is 30.0nA which is using Tween-20 as the indicator with using KEITHLEY 2450 as the measuring instrument of the current. Based on figure 8, the experiment are using Probe as a cut-off point too determined the target, non-compliment or compliment. If the target are lower than Probe it means non-compliment and if the target are higher than Probe it means compliment but the target compliment must be above 20nA. This is because when using the Probe as cut-off point all the result is different than other result which is lower value of measurement are obtain. But it is acceptable because it still follow the trend. Sample 1 until 3 is non-compliment target while sample 4 to sample 7 is compliment target. The outcome can be clearly identified that the noncomplementary target sample is below the Probe Cut-Off point while complementary target is above the Cut-Off point. The result obtained is accurate which is the complementary and noncomplementary target can be analysed clearly in using general Probe Current (A) value that is 20nA. See the results of the electrical measurements of selectivity for the complement and noncomplement targets of the COVID-19 samples in Figure 9. To facilitate interaction between the organic and inorganic surfaces of an RNA of covid probe, APTES is functionalized on the surface of Al IDE. An amine group, which predominantly retains positively charged ions, is present in APTES, the binding agent. The active area of the IDEs was doused with 2µl of 2% APTES to initiate the salinization process. Results show that dropping the APTES on the surface of the Al IDEs causes the current to continue increasing. The value, 4.87 nA, is shown by the current collected at 1 V. The Covid RNA probe was then dropped on top of the APTES layer to complete the immobilization procedure; this layer serves as a bio-receptor that can catch specific target complementary RNA. The 10µl of covid probe has been functionalized and immobilized on the APTES surface. Based on the result, current captured at 1V for covid probes shows 15.90nA. After the covid Probe, the Tween-20 will drop function as blocking agents it also react as to protect the RNA from contamination. According to the data presented in figure 4.9, the current measured at 1V for Tween-20 is 21.9nA. The non-complementary target depicted in the graph represents a current measurement of 1V, signifying that the non-complementary RNA is unable to connect with the immobilized RNA probes. Furthermore, they are likewise incapable of binding with Tween-20. The non-complement target exhibits a notable disparity in I-V characteristics at 1V when compared to immobilized RNA COVID probes. Consequently, it is verified that the sensor functioned effectively with the designated target. Based on result show the non-compliment are 13.2nA. The complement target shows the I-V measurement which target 10µL of covid-19 higher than Tween-20 it means it can detect the target, the result show the value of compliment is 49.30nA.

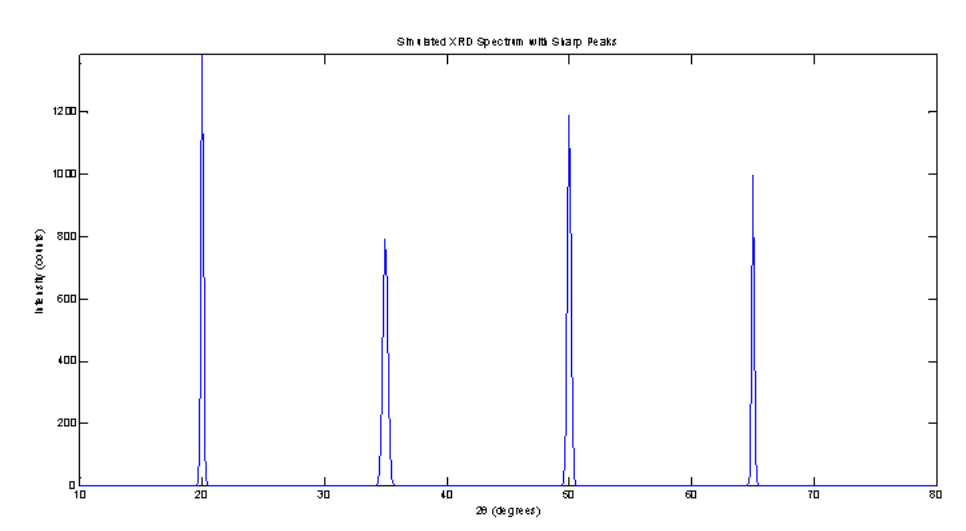


Figure 3: XRD spectrum characteristic diffraction pattern by introducing sharp peaks at specific 2-theta values, which correspond to diffraction angles of the IDE surface

The XRD spectrum characteristic diffraction pattern by introducing sharp peaks at specific 2-theta values, which correspond to diffraction angles. These peaks, defined using Gaussian functions, represent crystallographic planes with intense diffraction. The first peak at 20 degrees has the highest intensity of 1500 counts, showing a strong and narrow response with a small standard deviation, resulting in a sharp peak. This sharpness indicates a highly crystalline material with a specific and well-defined atomic arrangement. The use of small standard deviations in the Gaussian functions emphasizes the sharpness of the peaks, mimicking real XRD patterns seen in well-ordered crystal structures. The second peak at 35 degrees, with an intensity of 800 counts, is slightly broader due to a larger standard deviation compared to the peak at 20 degrees. The broader peak suggests a less intense diffraction event, possibly representing a different crystallographic plane with lower atomic density or weaker interactions with the X-ray beam. The third peak, at 50 degrees with 1200

counts, strikes a balance between intensity and sharpness, implying a moderately intense diffraction from a plane with medium atomic density. The placement of these peaks at regular intervals captures the essence of XRD analysis, where different atomic planes reflect X-rays at different angles. The final peak, located at 65 degrees with an intensity of 1000 counts, is sharp again, reinforcing the idea of a well-ordered structure that reflects the X-ray beam at a high angle. The combination of all four peaks forms the complete XRD spectrum, where the distinct sharp peaks reflect the material's crystallinity. The absence of gridlines in the plot enhances the focus on the peak shapes and their intensities, which are crucial for identifying material properties in FTIR analysis Figure 4. This simulated spectrum is typical of highly crystalline materials, where the presence of multiple sharp peaks corresponds to distinct lattice planes, allowing researchers to deduce structural information about the material.

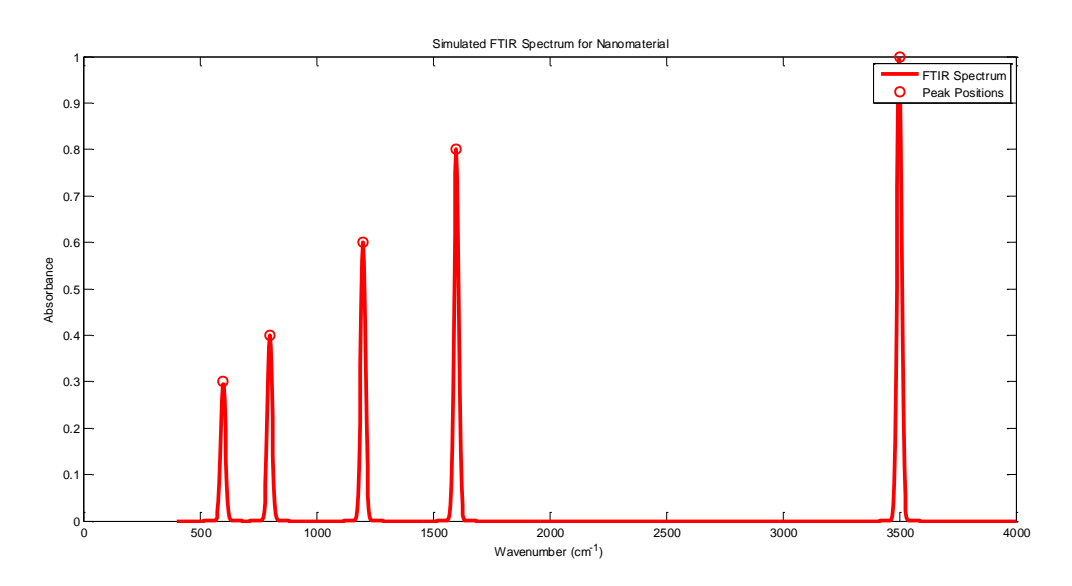


Figure 4: Ftir spectrum, where the distinct sharp peaks reflect the material's crystallinity

Figure 5 compares the current values measured at different time intervals (10 to 60 minutes) for four different experimental conditions Figure compares the current values measured at different time intervals (10 to 60 minutes) for four different experimental conditions: APTES+Probe, Complementary DNA, Mismatched DNA, and APTES+Probe+Tween-20. The APTES+Probe condition represents the baseline current generated by the interaction between the surface probe and the APTES (3-aminopropyltriethoxysilane) linker. Initially, at 10 minutes, the current is highest at 2.97E-08 A and decreases progressively to 4.71E-09 A by 60 minutes. This decline suggests a timedependent interaction that reduces current generation as the surface becomes saturated or the interaction reaches equilibrium. The Complementary DNA condition shows a slightly higher initial current of 3.10E-08 A compared to APTES+Probe, indicating that the hybridization of complementary DNA strands enhances the surface interaction, leading to a higher electrical response. However, like the APTES+Probe condition, the current declines over time, reaching 4.90E-09 A at the 60-minute mark. This decrease is likely due to a reduction in available hybridization sites or saturation of DNA binding, which reduces the overall current. In contrast, the Mismatched DNA condition starts with a lower current of 2.50E-08 A at 10 minutes, demonstrating weaker interactions due to mismatched base pairs that do not form stable hybridization complexes. The current also decreases steadily over time, reaching 4.50E-09 A at 60 minutes.

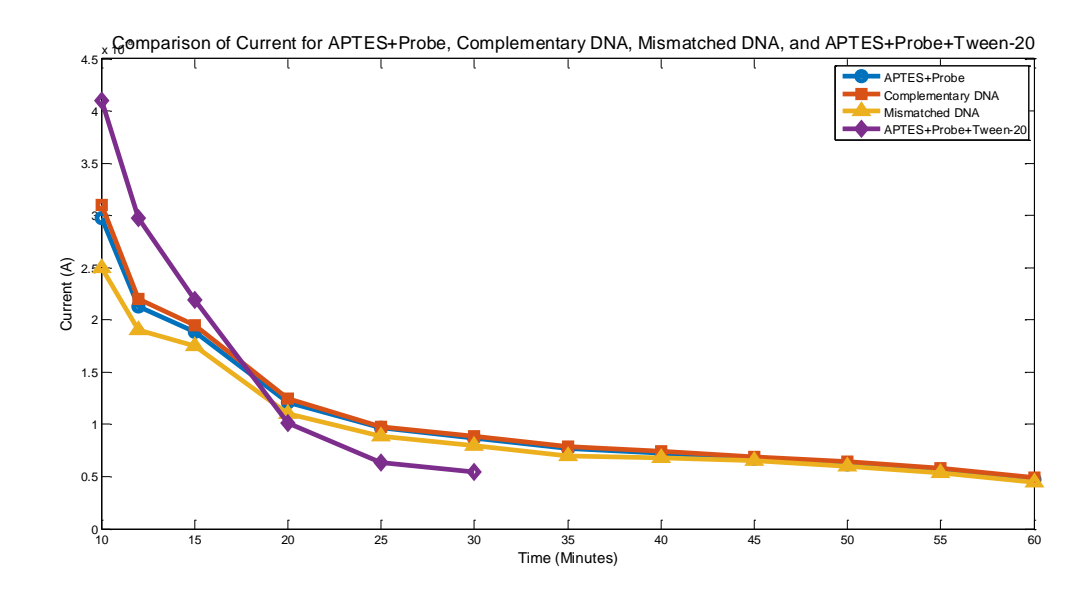


Figure 5. compares the current values measured at different time intervals (10 to 60 minutes) for four different experimental conditions: APTES+Probe, Complementary DNA, Mismatched DNA, and APTES+Probe+Tween-20

The lower overall current compared to the Complementary DNA condition highlights the specificity of DNA hybridization, where mismatched sequences lead to weaker and less stable interactions, thus generating less current. The APTES+Probe+Tween-20 condition shows the highest initial current of 4.10E-08 A at 10 minutes. However, it experiences a much steeper decline, dropping to 5.42E-09 A at 30 minutes, after which data is not available for later time points. Tween-20, a surfactant, likely affects the surface interaction by enhancing the probe's accessibility or reducing surface tension, leading to a higher initial current. However, the sharp decline suggests that Tween-20 may cause instability in the surface interaction over time, possibly disrupting the probe or DNA interactions at later stages.

4. Conclusion

The results of this study show that Tween-20 is the only thing that increased the amount of the desired DNA that the biosensor picked up. Primarily, Tween-20 enhanced current measurement by the combined APTES + Probe only, with currents increasing from $\delta 2.97$ E-08 A to 4.10 E-08 A (10 minutes). This enhancement simulates Tween-20, which could reduce unspecific interactions, thus obtaining higher biosensor sensitivity in this domain. The reduction of the present values for APTES+Probe and APTES+Probe+Tween-20 over time represents the stabilization of the biosensor, as well as the possible loss of signal with time. By the time we added Tween-20, after 30 minutes, we had a current of only 5.42E-09 A compared with the current of APTES+Probe only, 4.71E-09 A, and that of the complementary DNA, 4.90E-09 A, which shows the Tween-20 begins to inactivate. The biosensor generated higher current responses for complementary DNA than for mismatched DNA, proving that it distinguished between specific and non-specific interactions. When Tween-20 is used for detection, it is clear that it reduces non-specific binding, which leads to better performance. While Tween-20 is beneficial when mid- to long-term applications are warranted, its decreased ability to function effectively over time indicates a need for further optimization [21]. In conclusion, adding Tween-20 to a biosensor makes it work better, and this study shows that it is more sensitive and specific to complementary DNA identification. Further investigations on Tween-20 improvements and other modifications are justified to sustain high performance over longer detection times.

References

- 1. Afnan Uda, M. N., Bahari Jambek, A., Hashim, U., Uda, M. N. A., Parmin, N. A., Bakar, A. H. A., Anuar, A., Bakar, M. A. A., & Sulaiman, M. K. (2020). Design 5.0 μm Gap Aluminium Interdigitated Electrode for Sensitive pH Detection. *IOP Conference Series: Materials Science and Engineering*, 864(1), 0–7. https://doi.org/10.1088/1757-899X/864/1/012178
- 2. Afnan Uda, M. N., Jambek, A. B., Hashim, U., & Uda, M. N. A. (2020). Development of Voltage Amplifier Electronic Reader for Multiplex Detection of Two Electrode Electrical Biosensors. *IOP Conference Series: Materials Science and Engineering*, 743(1). https://doi.org/10.1088/1757-899X/743/1/012019
- 3. Afnan Uda, M. N., Parmin, N. A., Jambek, A. B., Hashim, U., Uda, M. N. A., Shaharuddin, S. N. A., & Adam, H. (2020). Nano-micro-mili Current to Mili Voltage Amplifier for Amperometric Electrical Biosensors. *IOP Conference Series: Materials Science and Engineering*, 743(1). https://doi.org/10.1088/1757-899X/743/1/012021
- 4. Alahi, M. E., & Mukhopadyay, S. C. (2017). Detection Methodologies for Pathogen and Toxins: A Review. *Sensors*, 17(8), 1885. https://doi.org/10.3390/s17081885
- 5. Alves, J., & C, R. De. (2021). *Journal Pre-proof. September 2020*. https://doi.org/10.1016/j.ijid.2021.01.001
- 6. Center for Disease Control. (2020). What you should know about COVID-19 to protect yourself & other. *Cdc*, 314937. https://www.cdc.gov/coronavirus/2019-ncov/download/2019-ncov-factsheet.pdf
- 7. Chakraborty, M., & Hashmi, M. S. J. (2017). Overview of Biosensor & Devices. *Reference Module in the Materials Science & Materials Engineering*. https://doi.org/10.1016/b978-0-12-803581-8.10316-9
- 8. Crowther, J. (2008). Enzyme Linked Immunosorbent Assay (ELISA). *Molecular Biomethod Handbook: Second Edition*, 657–682. https://doi.org/10.107/978-1-6327-375-6-37
- 9. Danny Jost. (2019). *What is a chemical sensor? | FierceElectronics*. https://www.fierceelectronics.com/electronics/what-a-chemical-sensor
- Gorbalenya, A., Baker, S., Baric, R., de Groot, R., Drosten, C., Gulyaeva, A., Haagmans, B., Lauber, C., Leontovich, A., Neuman, B., Penzar, D., Perlman, S., Poon, L., Samborskiy, D., Sidorov, I., Sola, I., & Ziebuhr, J. (2020). Severe acute respiratory syndrome-related coronavirus: The species and its viruses a statement of the Coronavirus Study Group. *Nature Microbiology*. https://doi.org/10.1101/2020.02.07.937862
- 11. Hoffman, W. L., & Jump, A. A. (1986). Tween 20 removes antibodies & other proteins from nitrocellulose. *Journal of Immunological Methods*, 94(1–2), 191–196. https://doi.org/10.1016/022-179(86)90232-2
- 12. Jayanath, N. Y., Nguyen, L. T., Vu, T. T., & Tran, L. D. (2018). Development of a portable electrochemical loop mediated isothermal amplification (LAMP) device for detection of hepatitis B virus. *RSC Advances*, 8(61), 34954–34959. https://doi.org/10.1039/c8ra07235c
- 13. Keithley Instruments. (2017). 2400 Graphical Series SMU / Tektronix. https://www.tek.com/keithleysourcemeasure-units/keithley-smu-2450series-sourcemeter
- 14. Khan, I., Saeed, K., & Khan, I. (2019). Nanoparticles: Properties, applications and toxicities. *Arabian Journal of Chemistry*, *12*(7), 908–931. https://doi.org/10.1016/j.arabjc.2017.05.011

- 15. Koli, D. K., Agnihotri, G., & Purohit, R. (2014). A Review on Properties, Behaviour and Processing Method for Al- Nano Al ₂ O ₃ Composites. *Procedia Materials Science*, *6*, 567–589. https://doi.org/10.1016/j.mspro.2014.07.072
- 16. Korotcenkov, G. (2014). Volumes 1 6 Ghenadii Korotcenkov (ed .). January 2011, 1–6.
- 17. Lanciki, A. (2020). Virus detection: Fast, sensitive, and cost-effective with electrochemical testing [White Paper]. *Metrohm AG*, 1–6.
- 18. Lisa Bender, C. N. C. M. A. & H. R. U. W. L. A. L., T. N. (UNICEF M. D. M. D. V. K. (WHO) and G. E. (IFRC). (2020). *Coronavirus & COVID-19 Overview: Symptoms, Risks, Prevention, Treatment & More*. https://www.webmd.com/lung/coronavirus
- 19. Mabe, T. L., Ryan, J. G., & Wei, J. (2018). Functional thin films and nanostructures for sensors. In *Fundamentals of Nanoparticles: Classifications, Synthesis Methods, Properties and Characterization*. Elsevier Inc. https://doi.org/10.1016/B978-0-323-51255-8.00007-0
- 20. Malorny, B., Anderson, A., & Huber, I. (2007). Salmonella Real-time PCR-nachweis. *Journal Fur Verbraucherschutz Und Lebensmittelsicherheit*, 2(2), 149–156. https://doi.org/10.1007/s00003-007-0167-x
- 21. Mitsuhiro Ebara. (2016). *Biomaterials Nanoarchitectonics Google Buku*. https://books.google.com.my/books?hl=id&lr=&id=drl0BgAAQBAJ&oi=fnd&pg=PP1&dq=A kifumi+Kawamura,+Takashi+Miyata.+Biosensors.+Mitsuhiro+Ebara.++++++++Biomateria ls+Nanoarchitectonics.+William+Andrew+Publishing,+2016:+157-+++++++++176.&ots=bibf15283Y&sig=pAx-qUmgGcB-dLG1RDXUtw-OZdk&redir_esc=y#v=onepage&q&f=false
- 22. Moulahoum, H., Ghorbanizamani, F., Zihnioglu, F., Turhan, K., & Timur, S. (2021). How should diagnostic kits development adapt quickly in COVID 19-like pandemic models? Pros and cons of sensory platforms used in COVID-19 sensing. *Talanta*, 222(August 2020), 121534. https://doi.org/10.1016/j.talanta.2020.121534
- 23. Mulaa, F. (2011). *Biosensors in: Handbook of Food Safety Engineering*. http://erepository.uonbi.ac.ke/handle/11295/17555
- 24. Murphy, N. M., McLauchlin, J., Ohai, C., & Grant, K. A. (2007). Construction and evaluation of a microbiological positive process internal control for PCR-based examination of food samples for Listeria monocytogenes and Salmonella enterica. *International Journal of Food Microbiology*, 120(1–2), 110–119. https://doi.org/10.1016/j.ijfoodmicro.2007.06.006
- 25. N. Lehman. (2013). Ribozymes and Evolution Ribozymes and Evolution Ribonucleic Acid.
- 26. Parmin, N. A., Hashim, U., Hamidah A Halim, N., Uda, M. N. A., & Afnan Uda, M. N. (2020). Characterization of Genome Sequence 2019 Novel Coronavirus (2019-nCoV) by using BioinformaticTool. *IOP Conference Series: Materials Science and Engineering*, 864(1). https://doi.org/10.1088/1757-899X/864/1/012168
- 27. Rahman, I. A., Jafarzadeh, M., & Sipaut, C. S. (2009). Synthesis of organo-functionalized nanosilica via a co-condensation modification using γ-aminopropyltriethoxysilane (APTES). *Ceramics International*, *35*(5), 1883–1888. https://doi.org/10.1016/j.ceramint.2008.10.028
- 28. Rajapaksha, R. D. A. A., Hashim, U., Afnan Uda, M. N., Fernando, C. A. N., & De Silva, S. N. T. (2017). Target ssDNA detection of E.coli O157:H7 through electrical based DNA biosensor. *Microsystem Technologies*, 23(12), 5771–5780. https://doi.org/10.1007/s00542-017-3498-2
- 29. Reen, D. J. (1994). Assay Immunosorbent. Walker J.M. (Eds) Basic Protein and Peptide Protocols. Methods in Molecular BiologyTM, 32.

- 30. Riquelme, M. V., Zhao, H., Srinivasaraghavan, V., Pruden, A., Vikesland, P., & Agah, M. (2016). Optimizing blocking of nonspecific bacterial attachment to impedimetric biosensors. *Sensing and Bio-Sensing Research*, 8, 47–54. https://doi.org/10.1016/j.sbsr.2016.04.003
- 31. Saeed, A. F. U. H., Wang, R., Ling, S., & Wang, S. (2017). Antibody engineering for pursuing a healthier future. In *Frontiers in Microbiology* (Vol. 8, Issue MAR, p. 495). Frontiers Media S.A. https://doi.org/10.3389/fmicb.2017.00495
- 32. Sensor, G., & Dahman, Y. (2017). Nanosensors * PROCESS ANALYSIS | Electroanalytical Techniques.
- 33. Smyrlaki, I., Ekman, M., Lentini, A., de Sousa, N. R., Papanicolaou, N., Vondracek, M., Aarum, J., Safari, H., Muradrasoli, S., Rothfuchs, A. G., Albert, J., Högberg, B., & Reinius, B. (2020). Massive and rapid COVID-19 testing is feasible by extraction-free SARS-CoV-2 RT-PCR. *MedRxiv*. https://doi.org/10.1101/2020.04.17.20067348
- 34. Stohlman, S. A., & Hinton, D. R. (2001). Viral induced demyelination. *Brain Pathology*, *11*(1), 92–106. https://doi.org/10.1111/j.1750-3639.2001.tb00384.x
- 35. Thivina, V., Hashim, U., Arshad, M. K. M., Ruslinda, A. R., Ayoib, A., & Nordin, N. K. S. (2016). Design and fabrication of Interdigitated Electrode (IDE) for detection of Ganoderma boninense. *IEEE International Conference on Semiconductor Electronics, Proceedings, ICSE*, 2016-Septe, 50–53. https://doi.org/10.1109/SMELEC.2016.7573588
- 36. Uda, M. N. A., Rajapaksha, R. D. A. A., Uda, M. N. A., Hashim, U., & Jambek, A. B. (2018). Selective detection of E.coli O157:H7 bacteria DNA using electrical based aluminium interdigitated electrode biosensor. *AIP Conference Proceedings*, 2045(Keithley 2450). https://doi.org/10.1063/1.5080840
- 37. Unicef, WHO, & IFRC. (2020). Key Messages and Actions for Prevention and Control in Schools. *Key Messages and Actions for COVID-19 Prevention and Control in Schools, March*, 13. https://www.who.int/docs/default-source/coronaviruse/key-messages-and-actions-for-covid-19-prevention-and-control-in-schools-march-2020.pdf?sfvrsn=baf81d52_4#:~:text=COVID-19 is 2019-nCoV.'
- 38. Union, I., Pure, O. F., & Chemistry, A. (1995). commission on general aspects of analytical chemistry classification and chemical characteristics of immobilized Classification and chemical characteristics of. 67(4), 597–600.
- 39. Van Der Hoek, L., Pyrc, K., Jebbink, M. F., Vermeulen-, W., Berkhout, R. J. M., Wolther, K. C., WertheimVan Dillen, P.ME., Kandorp, J., Spaargaren, J., & Berkhout, B. (2004). Identifications of a new human coronavirus. *Nature Medicines*, *10*(4), 368–373. https://doi.org/10.1038/nm1024
- 40. VisitFinland. (2007). About us About us. 138669. http://www.visitfinland.com/about-us/
- 41. Vlamidis, Y., Gualandi, I., & Tonelli, D. (2014). What is Biotechnology? Types and Applications Iberdrola. Journal of Electroanalytical Chemistry. https://www.iberdrola.com/innovation/what-is-biotechnology
- 42. Vlamidis, Y., Gualandi, I., & Tonelli, D. (2017). Amperometric biosensors based on reduced GO and MWCNTs composite for polyphenols detection in fruit juices. *Journal of Electroanalytical Chemistry*, 799(April), 285–292. https://doi.org/10.1016/j.jelechem.2017.06.012
- 43. Zhang, C. X. Y., Brooks, B. W., Huang, H., Pagotto, F., & Lin, M. (2016). Identification of surface protein biomarkers of Listeria monocytogenes via bioinformatics and antibody-based

- protein detection tools. *Applied and Environmental Microbiology*, 82(17), 5465–5476. https://doi.org/10.1128/AEM.00774-16
- 44. Alsahib, S.A., Thejeel, K.A."Synthesis of zinc oxide (ZnO) and study on mechanical properties of polymeric dental filling" International Journal of Drug Delivery Technology, 2021, 11(2), pp. 451–454
- 45. Thejeel, K.A."Synthesis and characterization of some new ibuprofen derivatives and study antibacterial activity"International Journal of Drug Delivery Technology, 2020, 10(3), pp. 454–458
- 46. Al-Sahib, S.A., Hitur Awad, S., Thejeel, K.A. "Synthesis, Characterization of Organic Nanoparticles of Oxadiazole Derivative". Journal of Physics: Conference Series, 2019, 1294(5), 052024